www.serd.ait.ac.th/reric

Solar Engine Application by using Concentrated Solar Energy

O. Aliman*1, L.C Chen*, C.S Lim*, I. Daut*, M. Isa* and M. R. Adzman*

Abstract- *A prototype of solar (heat) engine that has been developed and demonstrated in Universiti Teknologi Malaysia (UTM) is an adoption of modifying a commercial internal combustion engine into a Stirling engine driven by concentrated solar energy. The system which consisted of a new proposed rotation-elevation tracking mode heliostat – mechanically designed and developed for sun tracking and a computer designed optical receiver – fabricated multi-fold cones with mirror arrays to further concentrate of the sunlight, are specially developed for this experiment. In this paper, the development and feasibility test of the solar engine system will be reported. The 0.59% of overall efficientcy from solar energy to mechanical work produced in this experiment also will be discussed.*

Keywords - Solar Engine, Solar Thermal Energy, Stirling Engine, Heliostat, Optical Receiver.

1. INTRODUCTION

Converting solar energy into shaft power or mechanical power can be employed by any heat engine like single or multistage reciprocating steam engines, turbo-machines (using steam or organic vapours as working fluid), Stirling hot air engines or Brayton engines [1]. The selection of a particular solar (heat) engine depends on many parameters including power requirement (size), type of working fluid, temperature of operation and solar energy collection device. For low power requirement (<50kW), reciprocating engines, rotary displacement engines and Stirling hot air engines are potentially offer high efficiency [2]. In addition to Stirling hot air engine, it is a process that focused sunlight heats into the closed space containing a working fluid (normally air, helium or hydrogen), which then expands and forces down the piston and turning the flywheel clockwise. During the Stirling cycle, the variation of working space volume will induce cyclic pressure changes in the fluid while the displacement of fluid within the closed space will induce cyclic temperature changes [3].

Stirling engine was first invented by Robert Stirling of Scotland in 1816. By then, great development efforts to improve and increase its efficiency have been done by scientists and companies such Erricson, Farber, Prescott, Meijer, N.V. Philips Company, General Motors, etc. Thousands of experiments had been done which results the improvement from a low efficiency (up to 3%) to 38% [2].

In search of suitable application to match the current development of alternative method of sun tracking in UTM, Stirling engine has been chosen due to its high theoretical efficiency [4]. Therefore a new design of solar (heat) engine system utilizing Stirling cycle is developed. The system consists of a heliostat as sun tracking, an optical receiver as solar concentrator and a prototype Stirling engine.

*School of Electrical System Engineering, Kolej Universiti Kejuruteraan Utara Malaysia (KUKUM), 02600 Jejawi, Perlis, Malaysia

[1]Corresponding Author:
E-mail: omaraliman@kukum.edu.my

2. SOLAR ENGINE DEVELOPMENT

The system consists of a heliostat as sun tracking, an optical receiver as solar concentrator and a prototype Stirling engine.

Heliostat

The proposed alternative heliostat tracking mode so-called rotation-elevation mode tracks the sun with two axes. The conceptual design of the heliostat with the first axis is aligned pointing towards the target is illustrated in Fig.1. The second axis is fixed respect to the reflector surface and orthogonal to the first axis. The reflective surface of heliostat embraces one master mirror at the centre and surrounded by the slave mirrors. All mirrors are arranged into rows and columns, where the number of rows and columns are normally identical. Therefore, every row or column can be controlled using a single driving device. In fact, there are two additional rotation axes for the slave mirrors. First axis is along horizontal direction of the frame and parallel with the elevation-axis. The slave mirrors grouped into rows can be rotated about the horizontal-axis. Second axis is along the vertical direction of the frame and orthogonal to the first axis. The slave mirrors arranged into columns are able to be rotated about the vertical-axis.

The primary tracking is to target the solar image of master mirror into a stationary receiver. Then, this image acts as a reference for secondary tracking where all the slave mirror images will be projected on it. In the primary tracking, the heliostat tracks the sun in two axes, which are rotation-axis and elevation-axis. Fig. 2 illustrates the rotation mode of the heliostat where (a) $\underset{\sim}{ON}$ is defined as the normal vector of the heliostat surface; $\underset{\sim}{OS}$ is the vector that points to the sun; $\underset{\sim}{OT}$ is the vector that points to a fixed target. (b) The rotation of the plane of reflection, that plane which contains the three vectors ($\underset{\sim}{OS}$, $\underset{\sim}{ON}$ and $\underset{\sim}{OT}$), during primary tracking. In the new reflection plane, the vector $\underset{\sim}{OS}'$ points to the new position of the sun and the vector $\underset{\sim}{ON}'$ is the reflector normal of the new orientation so that the sunlight is still reflected towards the target.

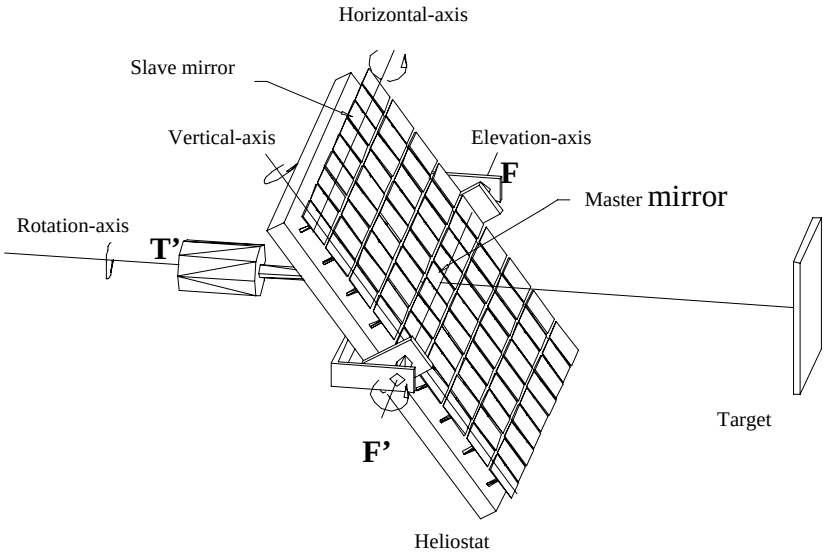

Fig. 1. Basic design of non-imaging focusing heliostat with two rotation axes of the frame and the other two additional axes of slave mirrors.

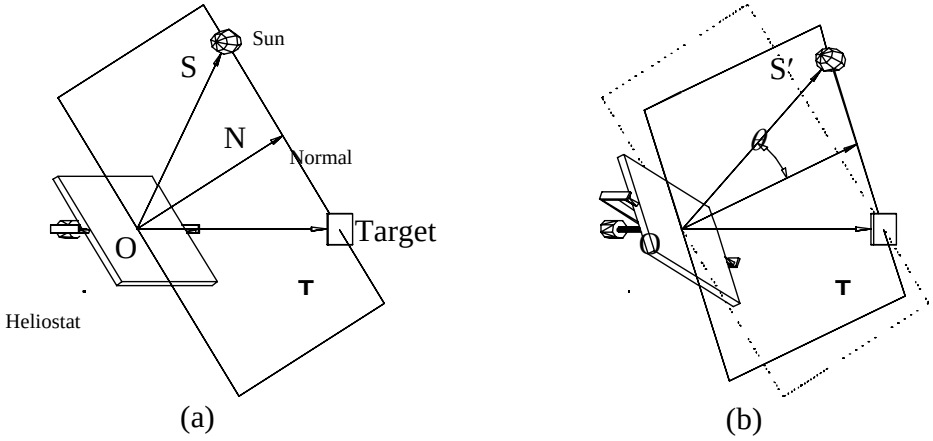

Fig. 2. Rotation modes of non-imaging focusing heliostat.

Rotation Movement - The heliostat has to rotate about the TT' axis so that the plane of reflection can follow the rotation of the vector $\underset{\sim}{OS}$. Therefore, as the sun moves through the sky from the morning to solar noon, the plane will rotate starting from horizontal and turning to vertical. The angular movement about this rotation axis is denoted as rotation mode.

Elevation Movement - The rotation of the heliostat about FF' axis (perpendicular to the plane) will adjust the reflector normal position within the plane until it bisects the angle between $\underset{\sim}{OS}$ and $\underset{\sim}{OT}$. As a result, the sunlight will be reflected onto the target. This angular movement depends on the incidence angle of the sun relative to the heliostat surface normal and it is denoted as elevation mode.

The heliostat used in this experiment has the reflecting area of $4m^2$. Assume a conservative solar heat flux density of $600W/m^2$, and an optical efficiency of 50% (by considering losses at heliostat, concentrator, scattering, cosine effect, etc.) the solar input power is estimated to be 1.2kW. The heliostat which consists of 25 mirrors can produce an average concentration of 25. With the aid of the secondary concentrator, overall average concentration ratio of 100 is achievable. The surface temperature of the hot cylinder is estimated to be around 600°C.

Optical Receiver

An optical receiver acting as solar concentrator comprises N folds of truncated cones that are combined together axially forming a "Manchurian Cap" as shown in Fig. 3 and Fig.4. Multi-fold cones are used to map incoming beams onto a line, which is relatively short compared to the axial length of the receiver. The design of this optical receiver is specific for the use with our newly developed heliostat and Stirling engine prototype. In our case, a 25-mirrors-heliostat concentrates all of the 25 sun images into 1 at the opening of the receiver. Such a focusing process results in non-parallel beams entering the receiver. Fig. 5 shows how a 9-mirrors-heliostat concentrates the sun images into the optical receiver.

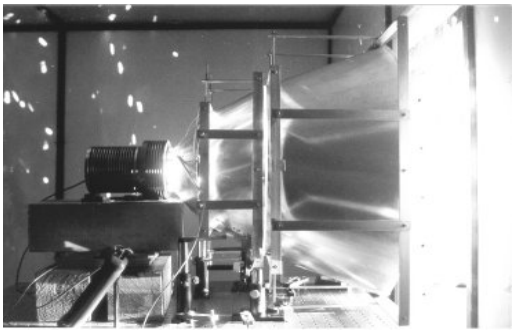

Fig. 3. Side view of a prototype receiver.

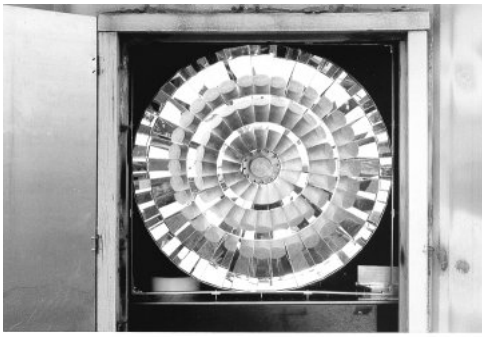

Fig. 4. Front view of a prototype receiver.

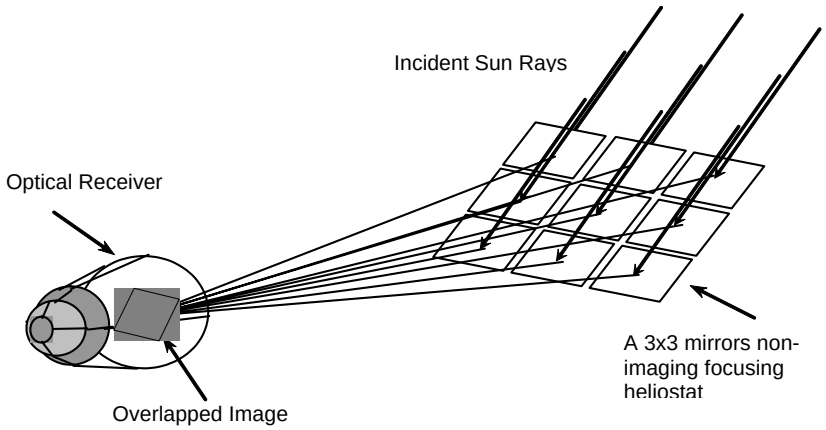

Fig. 5. A heliostat concentrates all of its 3x3 images into one at the opening of an optical receiver.

Besides that, the heliostat rotates throughout the day and that causes the image at the opening of the receiver to rotate with time. Meanwhile, the incident angle of the heliostat changes with days as the Earth revolves round the Sun. The change of incident angle will alter the size of the image formed at the receiver. All these non-parallelism and size variation of the image tremendously complicate the designing work of an optical receiver because the mathematical modeling is no longer straightforward. Therefore, a computational method has to be used to simulate the working condition of the heliostat-receiver system. By taking advantage of current advance of computing technology, CPU nowadays is fast enough to carry out finite ray tracing, which is almost impossible to be done by hand.

In order to model the working condition of a heliostat and an optical receiver, the sunlight that illuminates the system is approximated as composed of a finite number of discrete rays. The route of light rays from the heliostat to the receiver and, finally, to the absorber, is traced using a computer programme. However, many factors have to be considered in the modelling: (1) the movement of master mirror and slave mirrors during the course of tracking, (2) the declination of Sun, heliostat's latitude, heliostat's facing angle and target angle, (3) the reflectivity of the reflective surface, (4) the cosine effect of sun light, and (5) programme scalability for receiver design.

A vector-based ray tracing method is used to find the navigation route (in terms of bounce point) of each ray entering an optical receiver. Each sun image mapped to the opening of the receiver is treated as consisting of NxM rays where the value of N and M is determined by the required ray density, e.g. 800 rays per mirror side. Ray density for each image mapped to the opening is the same and user can set the density themselves. Meanwhile, a line vector describes each ray and rays that belong to the same image share the identical vector unit. The vector unit can be calculated from incident angle, target distance and mirror size. For simplicity, ray tracing is performed on group basis; rays with the same vector unit form a group. Thanks to the rotation modes of the proposed new technique of sun tracking (heliostat), symmetry effect can be used to reduce the number of group required to trace. In general, only N*(N/2+1) out of N*N group need to be traced and this results in tremendous execution speed boost. The route of each ray is traced and the hitting point on the absorber is recorded. The power received by the absorber can be deduced from the fraction of total rays hitting on the absorber and the total reflection loss.

Experiments have been carried out to measure the air temperature in the hot end of Stirling engine prototype. The engine is placed at the truncated root of an optical receiver as depicted in the picture of Fig. 3 and Fig. 4. The hot end cylinder of the engine protrudes towards the position that receives maximum irradiance. A K-type thermocouple is used to probe the air temperature. A maximum hot end air temperature of 616^{o}C had been recorded during a test on a clear day at 2.32p.m in UTM. The change of air temperature in the hot end of our Stirling during the course of heating is shown in Fig. 6. As shown in the graph, the air in the hot end can be heated up from 65^{o}C to 500^{o}C in a short time. Such a fast thermal response indicates that the heliostat and the optical receiver have made a high and uniform flux concentration on the hot end. At the same time, the air in hot end can still be heated up to 600^{o}C in 15 minutes.

Solar Engine

Modifying an internal combustion or diesel engine is not a new idea and the publication of demonstrating such idea was appeared as early as 1980s [5]. Believing that the commercial parts of better quality ensure a good performance of the engine, it was brought the adoption of modifying a commercial internal combustion engine into a Stirling engine for this experiment. Therefore, a Honda engine model 4S G150 was selected for modification.

Preliminary design is began with determine the expansion volume to suit the compression volume, which is fixed by the piston swept volume of the original IC engine. Although the practical output power of the engine usually much smaller than the prediction from the Schmidt analysis, it is very useful for the determination of the preliminary design parameters. Following results are illustrating the result from the Schmidt analysis.

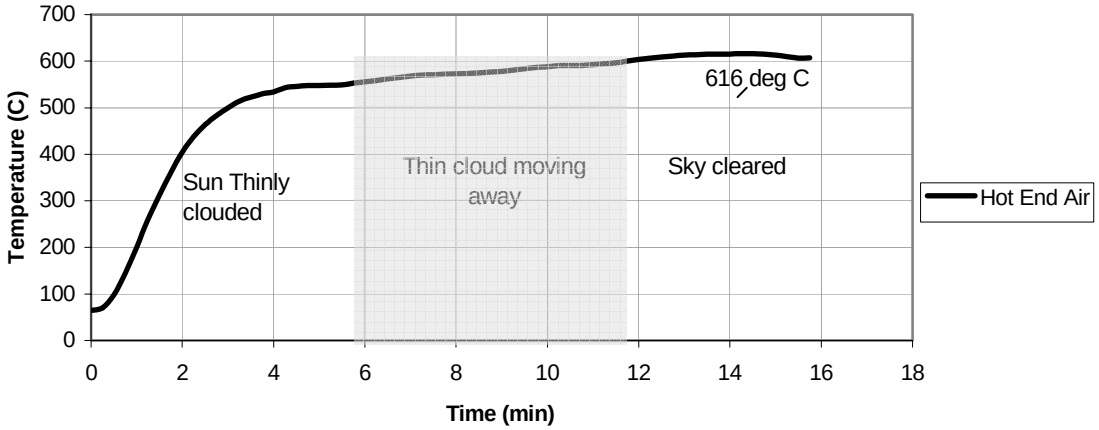

Fig. 6. Change of air temperature in a hot end during solar heating.

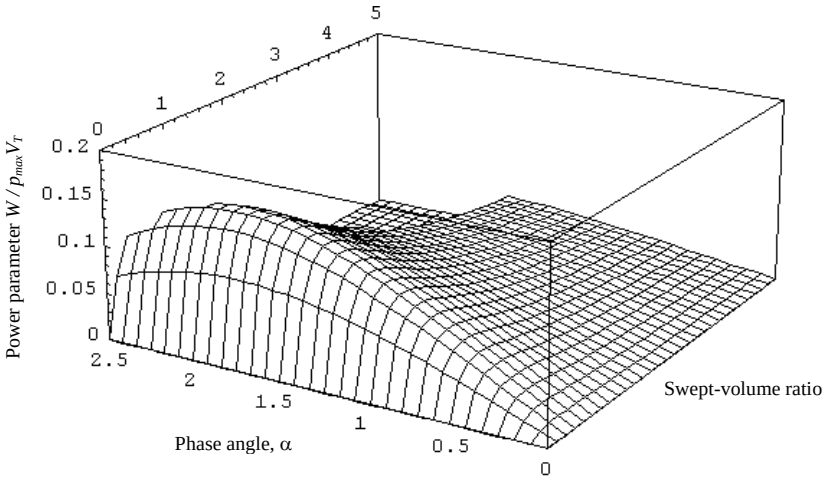

Fig. 7. The 3D plot of the power parameter in the function of phase angle, and swept volume ratio. The dead volume and the temperature ratio are assumed to be 0.5 and 0.36 respectively.

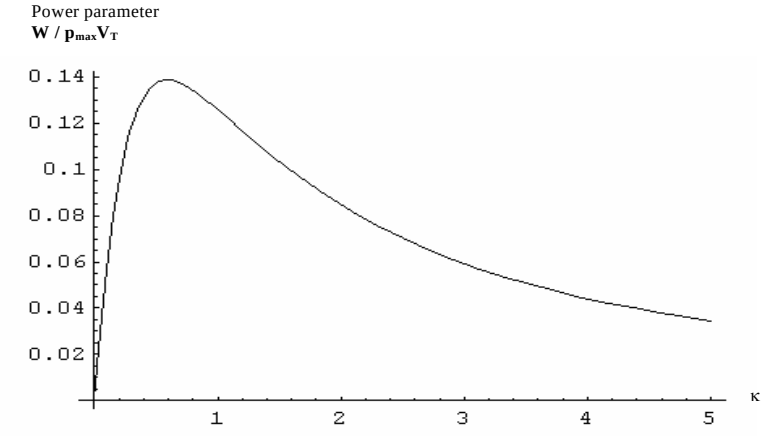

Fig. 8. The 2 D plot of the power parameter in the function of swept volume ratio when the dead volume ratio X = 0.5, and at the phase angle ~90°

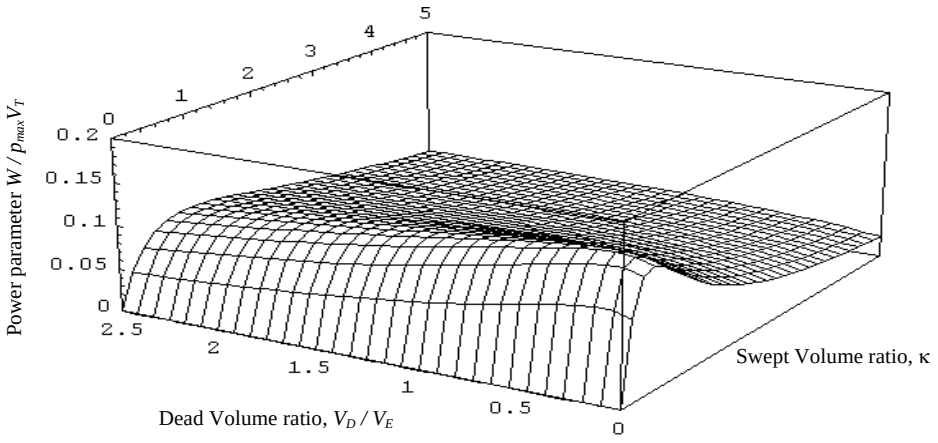

Fig. 9. The 3D plot of the power parameter in the function of dead volume ratio, and swept volume ratio. The phase angle and the temperature ratio are assumed to be 90° and 0.36 respectively.

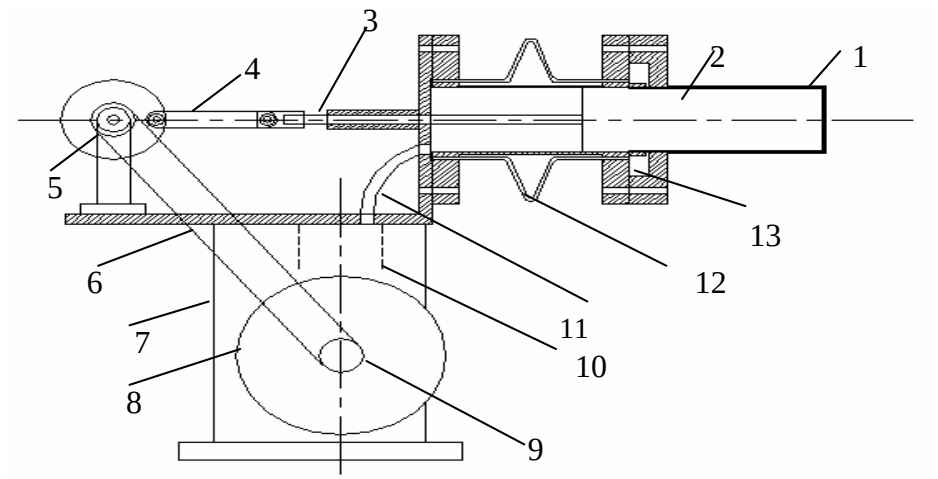

1 – Hot Cylinder
2 – Displacer
3 – Displacer rod
4 – Connecting rod
5 – Timing pulley
6 – Timing belt
7 – Original Crankcase
8 – Flywheel
9 – Timing pulley
10 – Piston Cylinder
11 – Connecting duct
12 – Cooling tube
13 – Regenerator

Fig. 10. The arrangement of the designed engine.

Fig. 7 to Fig. 9 illustrate the plot of engine power parameter, $W / p_{max} V_T$ in different conditions.

From the above analysis, the operating phase angle of the engine will be about 90°, and the maximum power occurs at the swept volume ratio of about 0.6.

In order to suit the optical power source, the engine is configured as a gamma type Stirling engine with the extension cylinder and the original piston cylinder separated at an angle of 90°. The extension cylinder will lie horizontally and parallel with the reflected sun ray the master mirror, whereas the original piston cylinder will be maintained as vertical. The arrangement of the modified engine is illustrated in Fig. 10.

The original piston cylinder was shown with dashed line in the figure and it is connected to the displacer cylinder via a copper-connecting duct. One timing pulley is attached to the main crankshaft, and the other to the displacer driving wheel. The timing pulley at the displacer driving wheel can be adjusted to the desired phase difference (90° which has been discussed in chapter 2) between the piston and the displacer. Together with the timing belt, the phase difference can be maintained even the engine is operated at high speed.

Learned from the initial experiment using pyramidal concentrator, the design approach for the new optical receiver is to reduce the multiple reflection by compound conic geometry. Fig. 11 illustrates the incoming sunlight is remapped onto the surface of the hot cylinder by the optical receiver. The ideal optical receiver reflects the incident sunray onto the target by single reflection because more reflections before hitting the target means more optical loss. But in practice the sunray from the heliostat is converging, as a result, not all the reflections is single reflection. At certain rim angle, sunlight rays ray may escape without hitting the target. The complete components in the design are shown in Fig. 12.

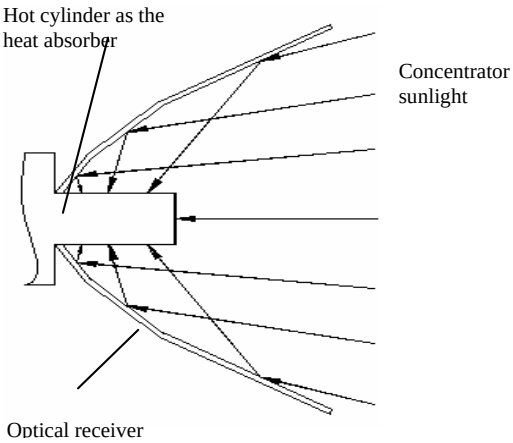

Fig. 11. The concentrated sunlight is reflected on the surface of the hot cylinder by an optical receiver.

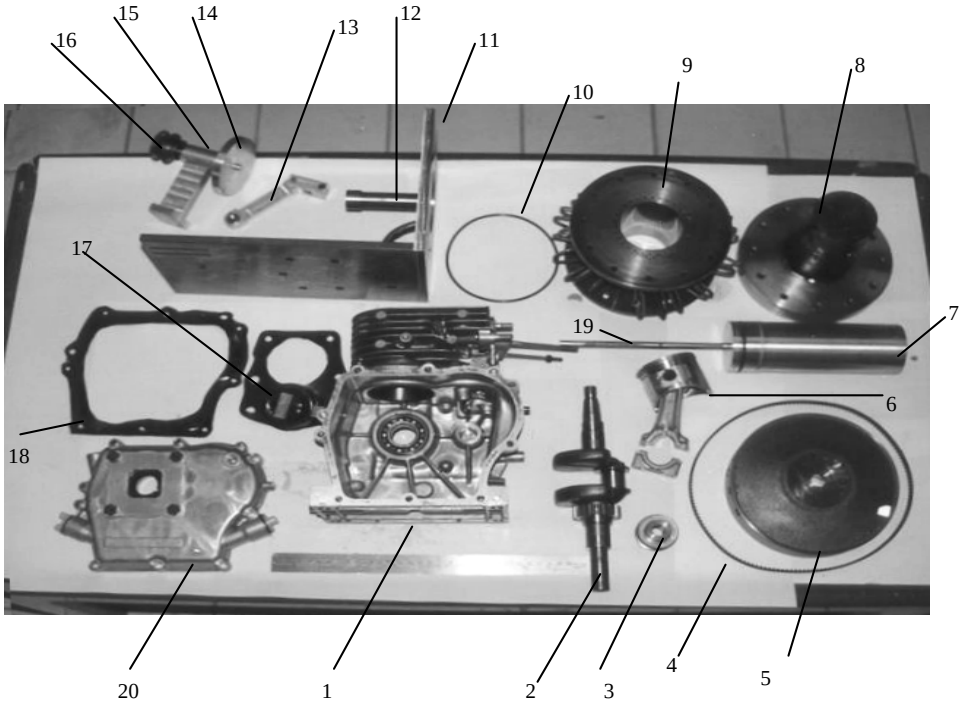

1 – Original crankcase
2 – Original crankshaft
3 – Timing pulley
4 – Timing belt
5 – Flywheel
6 – Original piston and the piston connecting rod
7 – Displacer
8 – Hot cylinder
9 – Cold cylinder
10 – Viton O-ring
11 – Mounting to the crankcase
12 – Displacer rod guiding bush
13 – Displacer connecting rod
14 – Displacer driving wheel
15 – Bearing house
16 – Timing pulley
17 – Rubber gasket for the crank case cover
18 – Rubber gasket substituting the original cylinder gasket
19 – Displacer rod
20 – Original crankcase cover.

Fig. 12. The complete components of the solar heated Stirling engine.

3. RESULT

Several preliminary testings were conducted before the solar experiment. In those tests, propane burner had been used as the input heat source to test the performance of the engine and the result are illustrated in Fig. 14 to Fig. 16. In addition, regenerator effect had been obeserved as illustrated in Fig. 13. It is learned from this experiment that regenarator could improve the engine performance by 40% in this experiment.

Obvious improvement in speed once the engine was charged with air at 1 bar difference with the atmospheric pressure as illustrated in Fig. 14.

The engine ran at 260 rpm on air at atmospheric pressure after ten minutes heated by propane burner. Then, the engine ran at average speed of 320 rpm after presurized at 1 bar and 2bars. However, the engine speed droped after further presurised to 3 bars.

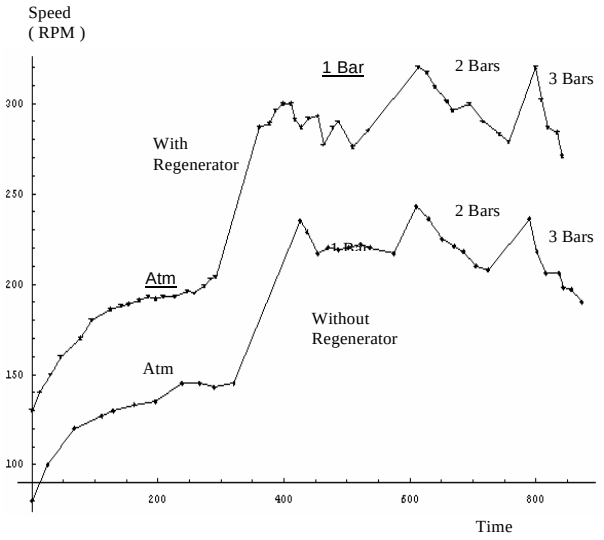

Fig. 13. RPM of the engine with and without the regenerator.

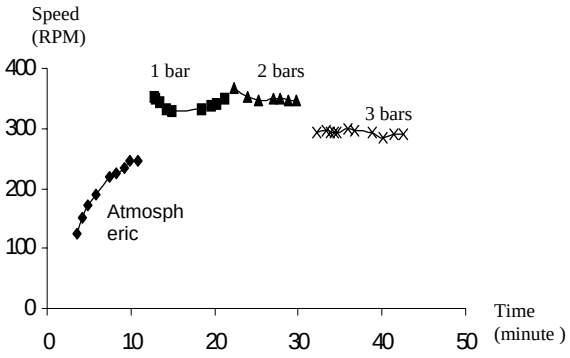

Fig. 14. Engine speed at different pressure.

The next experiment was done by using helium as the working gas. Fig. 15 shows the engine operated at a constant speed of 400rpm for one hour without showing obvious leaking.

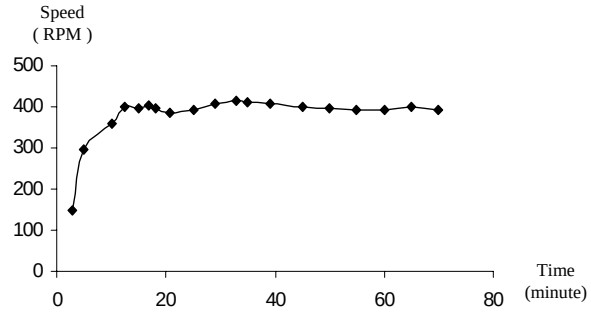

Fig. 15. The transient of the engine speed using Helium as the working gas at 1 bar.

The power of the engine was measured and the results was compared with the corresponding no load speed for different pressure in Fig 16.

The result shows that the engine power is still linearly proportional with the engine speed. In this experiment, it was obviously shown the improvement in power as well as in speed when the engine was pressurized from atmospheric pressure to 1 bar. However, it was learned from this experiment that neither further pressurizing the engine to 2 bars nor using the helium as the working gas gave a significant improvement in engine performance.

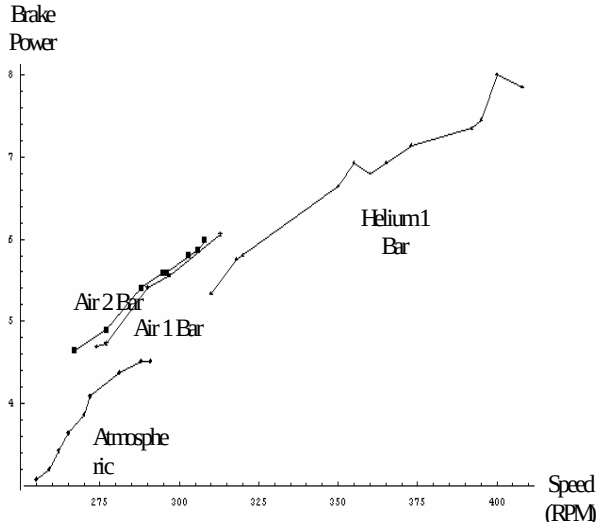

Fig. 16. Engine break power versus no load speed.

Next, the experiment was continued by replacing the propone burner with concentrated solar energy as the input source. A Pyrex beaker had been modified to cover the heat absorber in order to shield the heat exchanger from wind and ambient temperature. High temperature silicone was used to attached the glass cover to the engine hot cylinder and to seal the cold air from flowing in and the hot air from flowing out from the space between the heat absorber and the glass cover as illustrated in Fig. 17. The results for the engine running with and without the glass cover are shown in Fig. 18. It was learned from the experiment that, by covering the heat absorber would increase the engine speed about 10%.

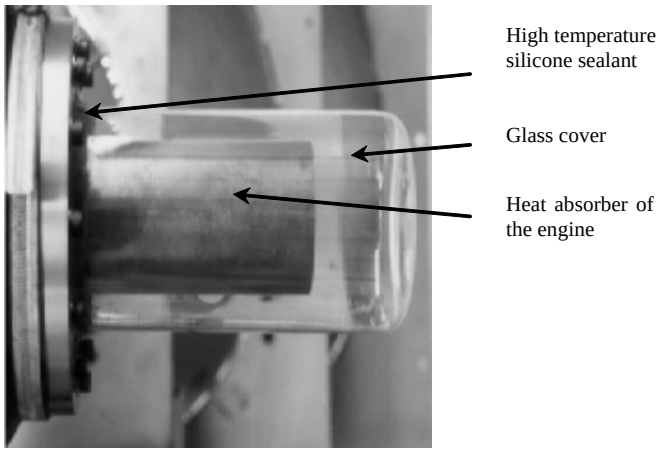

Fig. 17. The glass cover.

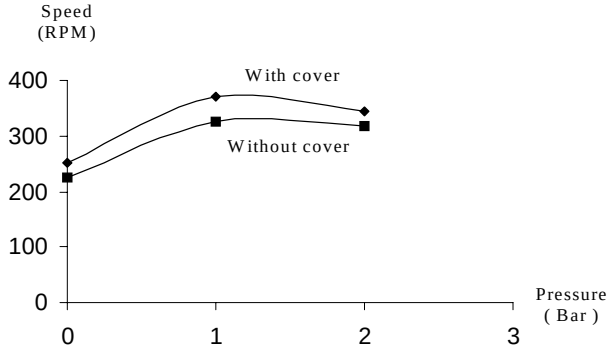

Fig. 18. The speed of the engine with and without the glass cover.

The experiment was repeated and Fig. 19 illustrates the result of experiment. It shows that, at 360rpm, the engine produce 8W mechanical power at 1 bar, and 10W at 2 bars. Indicates that higher pressure may relate to the power increase.

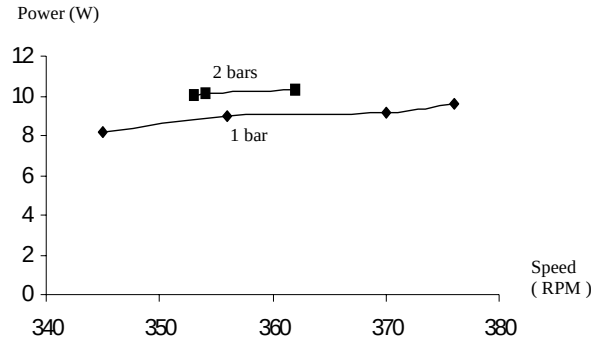

Fig. 19. Engine power versus speed using air as the working gas.

Due to weather problem during the experiment, it was continued at noon and the result is shown in Fig. 20.

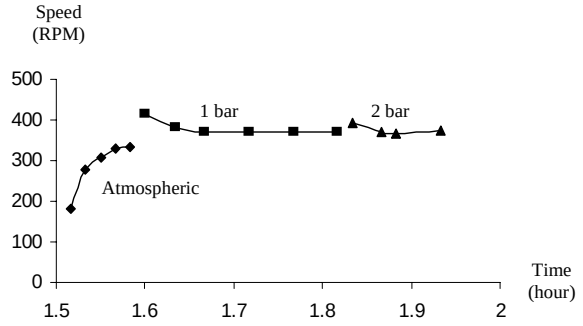

Fig. 20. The engine speed at different pressure measured in the afternoon.

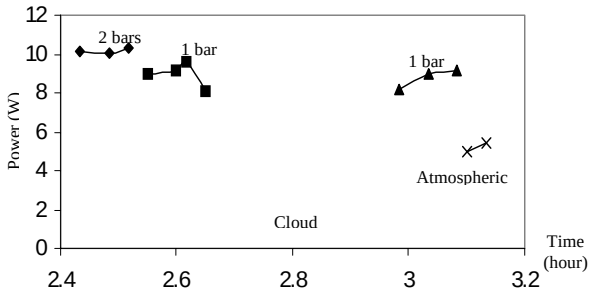

Fig. 21. The engine power at different pressure using solar power.

Fig. 21. illustrataes the measured brake power of the engine. The measurement was taken at time starting at 2.25pm. Using air as the working fluid, the measured brake power was about 10W at 2 bar, and 9W at 1 bar. Without pressurized, the brake power was around 5W. During the power measurement, the solar insolation was assumed to be constant except for the period when the sun was blocked by the cload.

The experimental engine produced a constant power of 10W at 2 bar with air as the working gas. Thus the overall efficientcy from solar energy to mechanical work produced in this experiment is only 0.59%.

4. DISCUSSION AND CONCLUSION

Solar Stirling Engine System

The merit of the system is that the target is stationary, thus the Stirling engine can have bigger size and heavier weight, hence higher power [6]. This is in contrast with the dish Stirling system where the engine is mounted and heated at the focal point of the parabolic dish. Thus, it requires a complicated lubrication system and limited size and weight. The major obstacle of the dish Stirling system is the uncertainty of the engine design and maintenance. Each engine failure or overhaul may require the engine to be uninstalled from the focal point, and the subsequent installation may result in optical realignment. Such operation would be laborious and costly.

Experimental Stirling Engine

The low 0.59% overall efficiency gained from the experimental Stirling engine cannot be used to reflect the performance of the matured commercial Stirling engine in such system. For low cost demonstration, the engine was not designed to operate at high pressure. Some of the design dimensions of the experimental engine have not been optimized especially the dead volume ratio. The design was also limited by the commercial parts of the internal combustion engine such as the bore stroke ratio of the piston. Instead of sophisticated heat exchanger design, the simplified version was adopted in the design to avoid complexity and trouble shooting in the demonstration.

5. CONCLUSION

The development and test demonstration of solar (heat) Stirling engine system powered by concentrated solar energy has successfully been done in UTM. Preliminary investigation of the performance of the solar flux receiver has been carried out using computer simulation. The simulation shows that optical heat exchanger should meet a minimum solar heat flux receiving area and operate at high concentration ratio while maintaining the sufficient heat transfer to the working fluid of the Stirling engine. It has been established in the literature that the mean concentration ratio of 2000 is necessary in order to attain high performance [7]. Although the concentration of the heliostat alone cannot meet the requirement but it is achievable with the low cost secondary concentrator. Compare with the established dish Stirling system, the fixed target characteristic of the system in UTM allows the heat engine to be bigger and heavier, thus offer an alternative to the conventional solar power system. With the support of efficient storage system, future development of the novel solar engine system in Malaysia is very much encouraging.

ACKNOWLEDGEMENTS

We acknowledge with many thanks to Prof. Y.T.Chen, and members of Solar Group which we formerly in the same team and effort, together struggling for the success of this research while we were in Universiti Teknologi Malaysia.

REFERENCES

[1] P.De. Laquil, D. Kearney, M. Geyer and R. Diner. 1993. Solar Thermal Electric Technology, *Renewable Energy* (Exercutive Editor : Laurie Burnham), Island Press, Washington: 213-296.

[2] H.P. Garg and J. Prakash. 2000. Solar Energy Fundamentals and Applications, 1st.Revised Edition, Tata McGraw Hill, New Delhi: 314-341.

[3] J. Corey.1989. Standards and Nomenclature for Reporting of Stirling Engine Performance. *IEEE, Paper No. CH2781-3/89/0000-2325*: 2325-2329.

[4] J.W. Sterns Jr., Y.S. Won, E.Y. Chow, P.T. Poon and R. Das. 1979. Solar Stirling Development, AIAA Terrestrial Energy Systems Conference, June 4-6, 1979, Orlando Florida.

[5] G. Walker. 1982. Future Coal-Burning Stirling Engine, *International Mechanical Engineering Publication*, 2.

[6] Y.T.Chen, K. K. Chong, Omar Aliman , T. P. Bligh1, L. C. Chen, Jasmy Yunus, K. S. Kannan, B.H. Lim, C. S. Lim, M. A. Alias, Noriah Bidin, Sahar Salehan, Shk. Abd. Rezan S.A.H., C. M. Tam And K. K. Tan. 2001. Non-Imaging Focusing Heliostat, *International Journal of Solar Energy, 71* (3):155-164.

[7] Thomas Keck, Wolfgang Schiel, Rainer Benz. 1990. *An Innovative Dish-Stirling System*, IECEC.